Supplementary Materials for

Intrinsically Self-Healable, Stretchable Thermoelectric Materials with Large Ionic Seebeck Effect

Zico Alaia Akbar,[a,b] Ju-Won Jeon,[b*] Sung-Yeon Jang[a*]

[a]School of Energy and Chemical Engineering, Ulsan National Institute of Science and Technology (UNIST), 50 UNIST-gil, Ulsan 44919, Republic of Korea

[b]Department of Chemistry, Kookmin University, 77 Jeongneung-ro, Seongbuk-gu, Seoul 136-702, Republic of Korea

***Corresponding author. Email: jwjeon@kookmin.ac.kr (J.W.J.); syjang@unist.ac.kr (S.Y.J.)**

Methods

Materials. Poly(2-acrylamido-2-methyl-1-propanesulfonic acid) (15 wt% in water, MW= 2,000,000), aniline, phytic acid (50 wt% in water), and ammonium persulphate were purchased from Sigma-Adrich.

Synthesis of PANI:PAAMPSA:PA ternary hybrid. For the preparation of PANI:PAAMPSA:PA dispersion, 10 g PAAMPSA aqueous solution, 0.2 g aniline, and 1 g phytic acid were mixed together and cooled at < 5^{o}C using an ice bath. Simultaneously, ammonium persulphate (APS) aqueous solution was prepared by adding 0.274 g of APS into 1 ml deionized water and cooled at < 5^{o}C. The APS solution was poured into the polymer mixture to initiate polymerization, and the reaction further proceeded for 12 h. The synthesized ternary hybrid can be readily used afterward. The composition of typical ternary hybrid is 9 wt% of PANI, 68 wt% of PAAMPSA, and 23 wt% of PA, respectively.

Film fabrication. The thin film samples were fabricated by drop-casting the polymer dispersion onto pre-cleaned glass substrates, followed by spin-coating. The thickness of the film was controlled by spin-coating speed and measured by alpha step. The thickness of the samples was 3-5 µm. The films were then directly heated on a hotplate for 5 mins at 60 ^{o}C. Then, 100 nm thick silver electrodes lines were deposited onto the film using a vacuum evaporator at the speed of 1.3 nm s^{-1}. The pressure of a vacuum base was maintained at 1×10^{-5} torr. The samples were kept in the humidity-controlled chamber before measurement. For the stretchable and self-healable experiments, the PANI:PAAMPSA:PA was deposited onto 3M substrate (3M-VHB-4910 tape) instead of glass substrates.

Seebeck coefficient measurement. The Seebeck coefficient of the samples was measured using a home-built Seebeck measurement setup using Agilent 34410A and Agilent 34970A, which were

controlled by a Labview software. Peltier devices, attached to an aluminum heat sink, were connected with Keithley 2400 as a current source to apply the temperature gradient on the sample (Fig. S11). T-type thermocouples (40 WG) connected to Keysight 34970A was used to measure the temperature of the samples. The silver paste was applied at the tip of the thermocouple, to ensure stable thermal and electrical contact between the thermocouple tip and silver electrodes. The Seebeck coefficient of the sample was obtained from the linear relationship between thermovoltage and temperature difference from the five different experiments with different temperature gradients. In order to standardize Seebeck measurement, the Seebeck coefficient of nickel plate was measured (Fig. S12), which is -19.96 μV K^{-1}. This is consistent with the literature.[1] The Seebeck coefficient of the samples was measured inside a humidity-controlled chamber, whose humidity can be adjusted ranging from 50% to 100% RH. The samples were stabilized for 15 min before any measurements. The stretching test was performed by stretching the thin film sample deposited on 3M-VHB-4910 substrates.

Electrical conductivity measurement. The ionic and electronic conductivities of the sample films were measured using impedance spectroscopy (COMPACTSTAT, IVIUM technologies) with the two-point probe. An AC voltage of 0.1 V was applied in the frequency range from 0.8 MHz to 0.1 Hz. The ionic resistance (R_i) and electronic resistance (R_e) are obtained by fitting the Nyquist plot with the equivalent circuit model (Fig. S8b). The electrical conductivity was calculated by $\sigma=d/(RA)$, where d, R, and A represents the distance between the two electrodes, the resistance, and the cross-sectional area of TE films, respectively. The thickness of the film was determined using alpha step profilometer (KLA-TENCOR). The electrical conductivity measurement was also performed inside a humidity-controlled chamber. Self-healing tests, otherwise stated in the

manuscript, were performed by cutting the thin film sample deposited on the 3M-VHB-4910 substrate.

The electrical conductivity of the stretched-sample is calculated by the following equation. Since the geometrical shape deformation would also affect the resistance, the real electrical conductivity can be estimated by subtracting the effect of resistance change caused by geometrical shape deformation (R_G/R_0),[2,3]

$$\sigma/\sigma_0 = (R_G/R_0)/(R/R_0)$$

where σ_0 is the initial electrical conductivity without strain, σ is the electrical conductivity at each strain level. R_G is the theoretical resistance from geometrical shape deformation under each strain based on the equation below, R_0 is the initial resistance without strain, and R is resistance, which was measured by EIS at the different strain level.

$$R_G/R_0 = (1+\varepsilon')/[(1-\varepsilon_{T1}(\varepsilon)')(1-\varepsilon_{T2}(\varepsilon)')]$$

where ε' is the fractional strain: $\varepsilon' = \varepsilon/100$ %. The term $(1 + \varepsilon')$ accounts for the increase in the length of the film when strained by ε'. The terms $(1-\varepsilon_{T1}(\varepsilon)')$ and $(1-\varepsilon_{T2}(\varepsilon)')$ account for the contraction in width and thickness with strain, respectively. The $\varepsilon_{T1}(\varepsilon)'$ describes the contraction in width (3M-VB-4910), while and $\varepsilon_{T2}(\varepsilon)'$ describes the contraction in thickness (PANI:PAAMPSA:PA) as a function of longitudinal strain. For isotropic samples, contraction of in width and thickness directions are the same. The transverse strains (width strain) of PANI:PAAMPSA:PA free-standing films and 3M-VB-4910 substrates were measured separately, as a function of longitudinal strain as plotted in Fig. S13. As can be seen in Fig. S13, PANI:PAAMPSA:PA is more easily contracted than 3M-VB-4910. Thus, for the contraction in width, the 3M-VB-4910's contraction ($\varepsilon_{T1}(\varepsilon)$), and PANI:PAAMPSA:PA's contraction ($\varepsilon_{T2}(\varepsilon)$) was used for thickness change.[3]

Thermal conductivity measurement. The thermal conductivity was calculated from the equation $k = C_p \rho D$, where C_p is the specific heat capacity, ρ is the density of the sample, and D is the thermal diffusivity. The out-of-plane thermal diffusivity was measured by laser flash analysis (LFA 467, NETZSCH) at 40% RH and 35ºC. The thermal diffusivity is described by $D = 0.1388\ d^2/t_{1/2}$, where d is the thickness of the sample, and $t_{1/2}$ is the time to reach the half-maximum temperature. The specific heat capacity was obtained using differential scanning calorimetry (DSC 200 F3, NETZSCH). At ambient conditions (~40% RH), the C_p of PANI:PAAMPSA:PA was determined to be 1.898 ± 0.088 J g^{-1} K^{-1}, while the D and ρ was determined to be 0.129 ± 0.005 mm^2 s^{-1} and 1.467 ± 0.011 g cm^{-3}, respectively, which resulted in the k of 0.358 ± 0.022 W m^{-1} K^{-1}. The thermal conductivity of the sample is dependent on the RH. The k values of the sample at various RHs were obtained using the following equation, $k_t = k_p ø_p + k_w ø_w$, where ø is volume fraction and the subscripts t, p, and w correspond to the hydrated PANI:PAAMPSA:PA, PANI:PAAMPSA:PA at RH 40%, and water, respectively. The volume fraction of the water at different RH % was calculated from the mass of absorbed water at each RH %.[4] The k value of water is 0.6 W m^{-1} K^{-1}. Free-standing films of the PANI:PAAMPSA:PA samples with a diameter of ~12.7 mm and thickness of ~ 1-2 mm was used for both LFA and DSC measurement.

To calculate the density of samples at RHs of 50% to 90%, the mass of the samples at each RH was first measured. The volume was estimated by considering the expanded volume due to water absorption at each RH%, as shown in the equation below,

$$V_{total} = V_{sample} + V_{water} = M_{sample}/\rho_{sample} + M_{water}/\rho_{water}$$

The V_{total} is the total volume at particular RH %, V_{sample}, M_{sample} , and ρ_{sample} are volume, mass, and density of the sample at 40% RH, respectively. V_{water}, M_{water} and ρ_{water} are volume, mass, and

density of the water at particular RH%. V_{water} is obtained by measuring the mass of the absorbed water of the samples at different RH % and divided by water density (1 g cm^{-3}). Therefore, the density of the sample at each RH % can be calculated by dividing the mass after the water absorption by V_{total} at each RH %.

Power output. The average power output is calculated based on the following equation:

$$P = \frac{E}{\Delta t} = \frac{\int V_{out} I dt}{\Delta t} = \frac{\int \frac{V_{out}^2}{R_{out}} dt}{\Delta t}$$

where V_{out} is the voltage observed in the external circuit, R_{out} is the resistance of an external resistor, and Δt is the time when the voltage decreased to zero.

Tensile stress tests. The tensile tests were carried out using a universal tensile meter (MTS QTest 25). The freestanding sample was fabricated by casting the polymer dispersion into a rectangular Teflon mold to obtain 10 × 30 mm rectangular-shaped films. The samples were dried at room temperature for 24 h. Prior to the measurement, the sample was placed in the chamber at the designated humidity levels for 1 h. The freestanding samples were held by pneumatic grip, and the gauge length was set to ~20 mm. The strain rate was 10 mm/min.

SEM, XPS, and UV-Vis measurement. SEM and EDS mapping were performed on a Hitach High-Technologies S-4800 cold FE SEM. For X-ray photoelectron spectroscopy (XPS), the PANI:PAAMPSA:PA dispersion was spin-cast onto a pre-cleaned silicon substrate, resulting in approximately 4-μm-thick films. XPS was carried out using an ESCALAB 250XI (Thermo Fisher Scientific), equipped with a high-performance Al Kα monochromatic X-ray source (15 kV, 10 mA). The base pressure was 1×10^{-9} Pa. UV–Vis spectra of the diluted PANI:PAAMPSA:PA dispersion were measured using a Mega-800 (Scinco) UV–Vis spectrophotometer.

Ionic thermoelectric capacitor. The PANI:PAAMPSA:PA thin-film ITEC device was characterized using the previously reported method as shown in Fig. 5b.[5] A four-stage thermocycle was applied to characterize heat-to-electricity conversion of the ITEC device at the RH of 70–80%.

In stage I, the temperature difference of 1.8 K was applied to the device. In stage II, the device was connected with an external load having a resistance of 8.2 kΩ while maintaining the same temperature difference in stage I (1.8 K). In stage III, the external load was disconnected, and the temperature gradient was removed from the device. In stage IV, the device was reconnected with the same external load (the 8.2 kΩ resistor). The thermovoltage output was recorded by an Agilent 34410A throughout the four-stage thermocycles, while the temperature difference was recorded using an Agilent 34970A. For the self-healing test, the razor blade was used to create the scratch of ~25 μm of PANI:PAAMPSA:PA thin film deposited on the glass substrate. The voltage profiles of the ITEC device were monitored before and after self-healing processes.

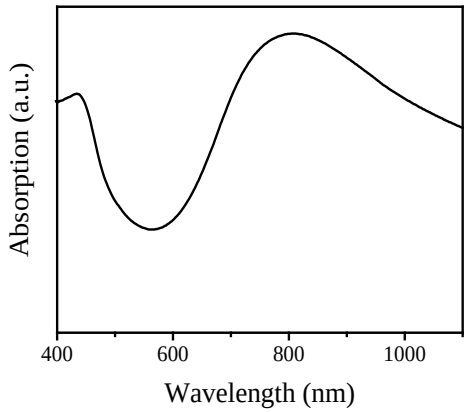

Fig. S1 UV–Vis spectrum of PANI:PAAMPSA:PA dispersion.

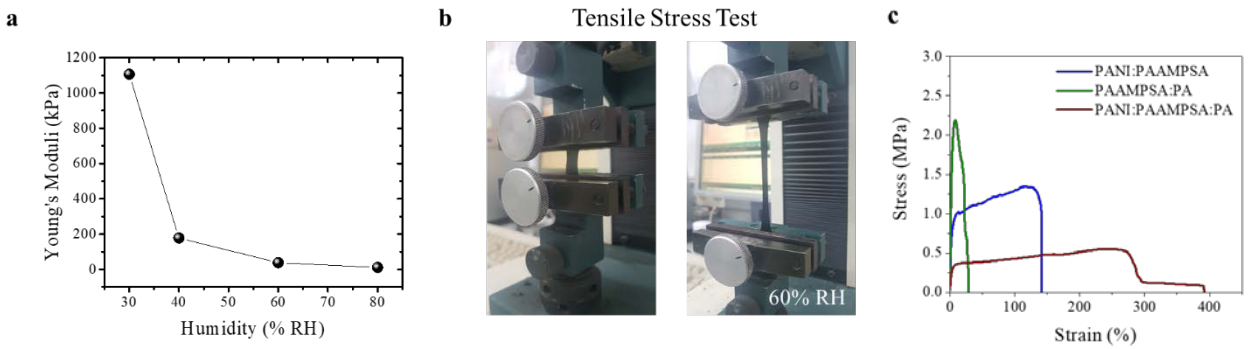

Fig. S2 (a) Young's Moduli of PANI:PAAMPSA:PA at different humidity levels. (b) Photographs of PANI:PAAMPSA:PA at initial and stretched conditions at 60% RH. (c) Stress-strain test result of PANI:PAAMPSA, PAAMPSA:PA, and PANI:PAAMPSA:PA samples at 40% RH.

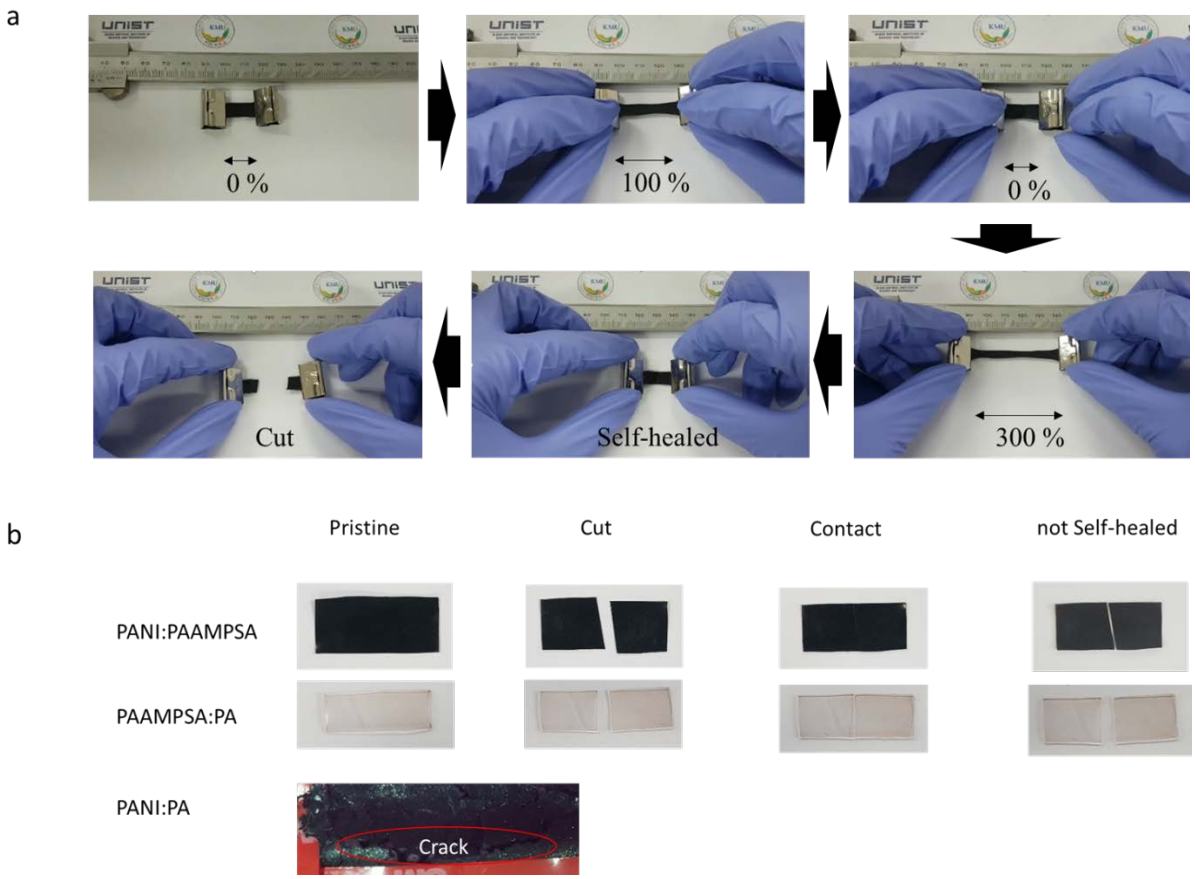

Fig. S3 Self-healing characteristics of (a) the ternary TE hybrid film at ambient condition (~50% humidity level) and (b) binary system samples: PANI:PAAMPSA, PAAMPSA:PA, and PANI:PA.

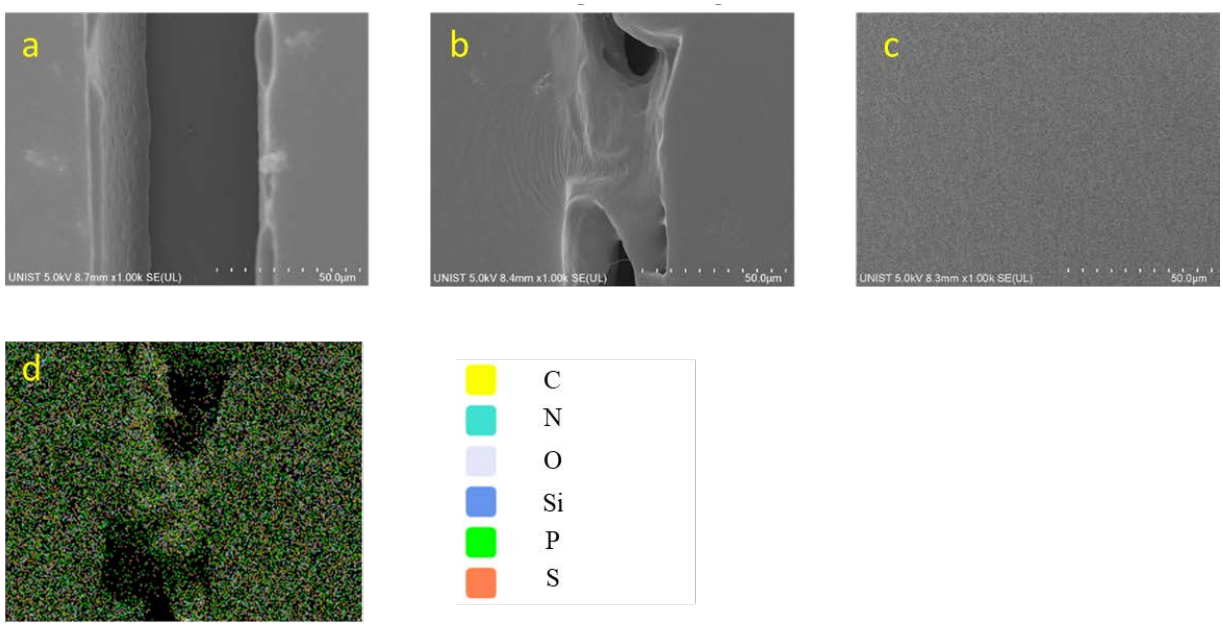

Fig. S4 SEM images of PANI:PAAMPSA:PA ternary film; (a) after cutting, (b) during self-healing, and (c) after self-healing. (d) EDS elemental mapping image of PANI:PAAMPSA:PA sample during self-healing process.

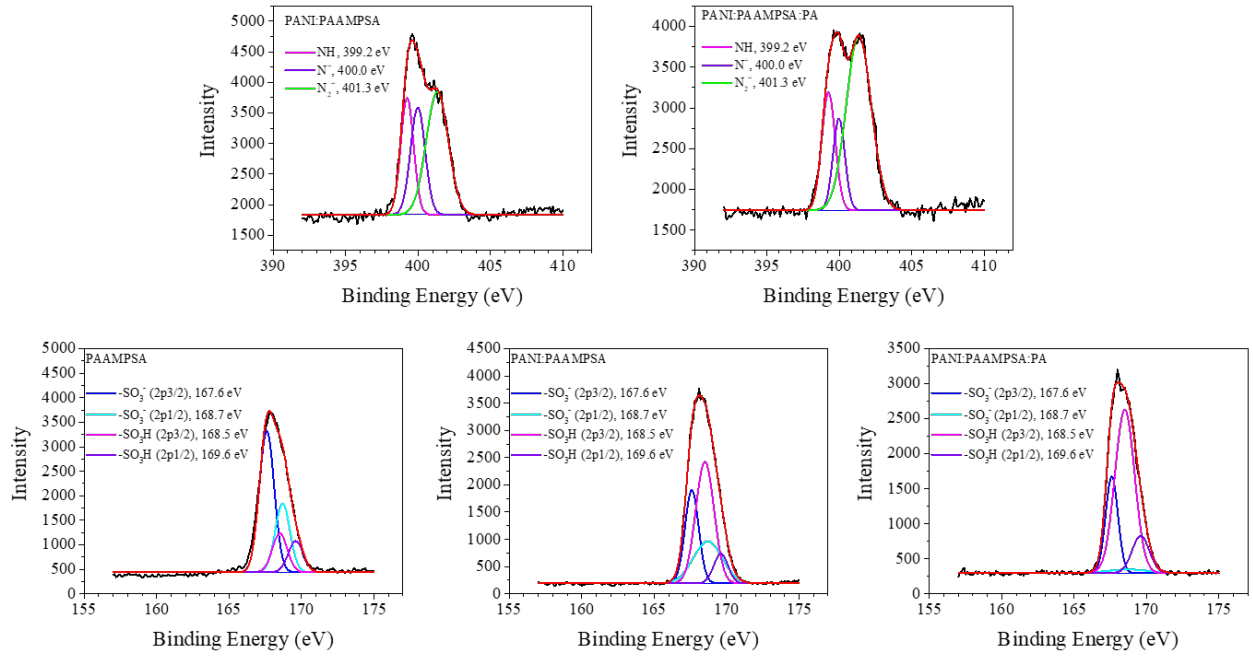

Fig. S5 High-resolution XPS spectra of PAAMPSA, PANI:PAAMPSA, and PANI:PAAMPSA:PA ternary hybrid with deconvoluted N 1s peaks and S 2p peaks.

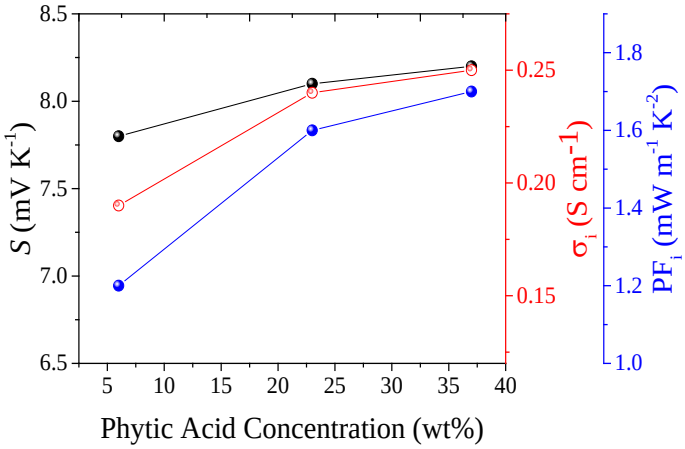

Fig. S6 Plots of thermoelectric properties of the TE hybrids with different PA content.

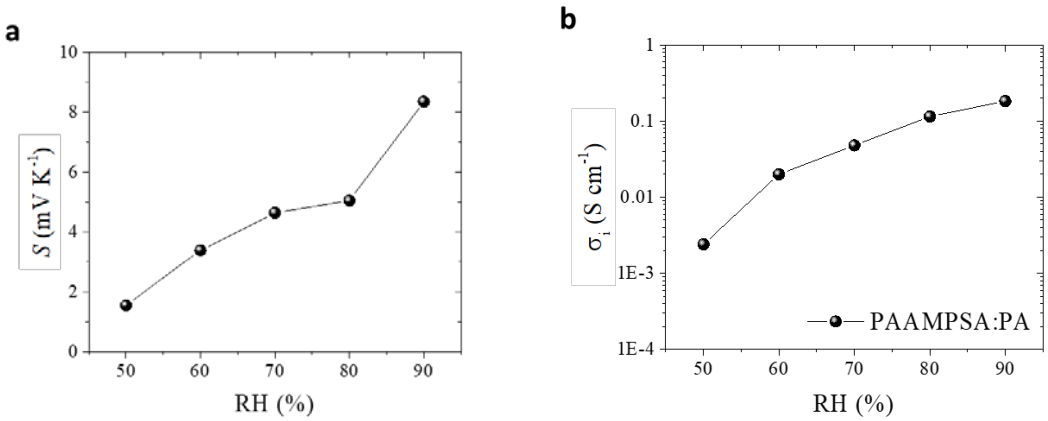

Fig. S7 (a) Seebeck coefficient and (b) ionic conductivity of PAAMPSA:PA at various RH.

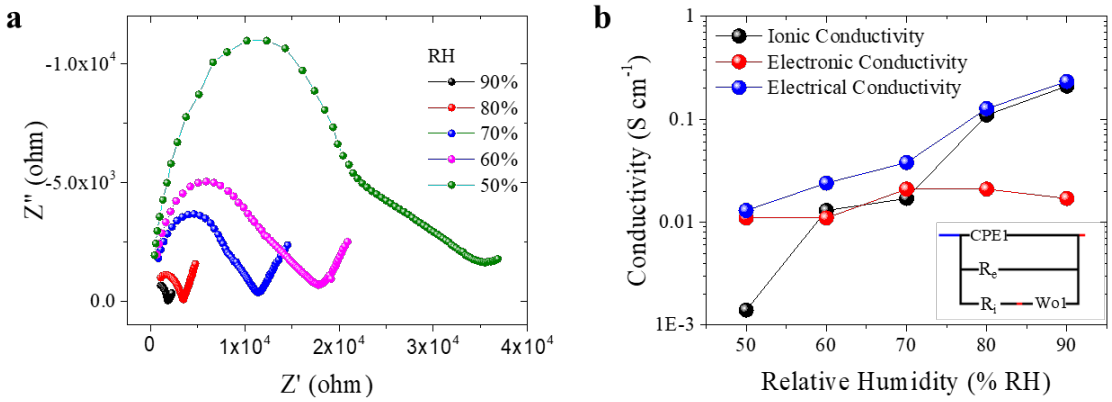

Fig. S8 (a) Nyquist plots and (b) ionic, electronic, and electrical conductivities of the TE hybrids at various humidity levels.

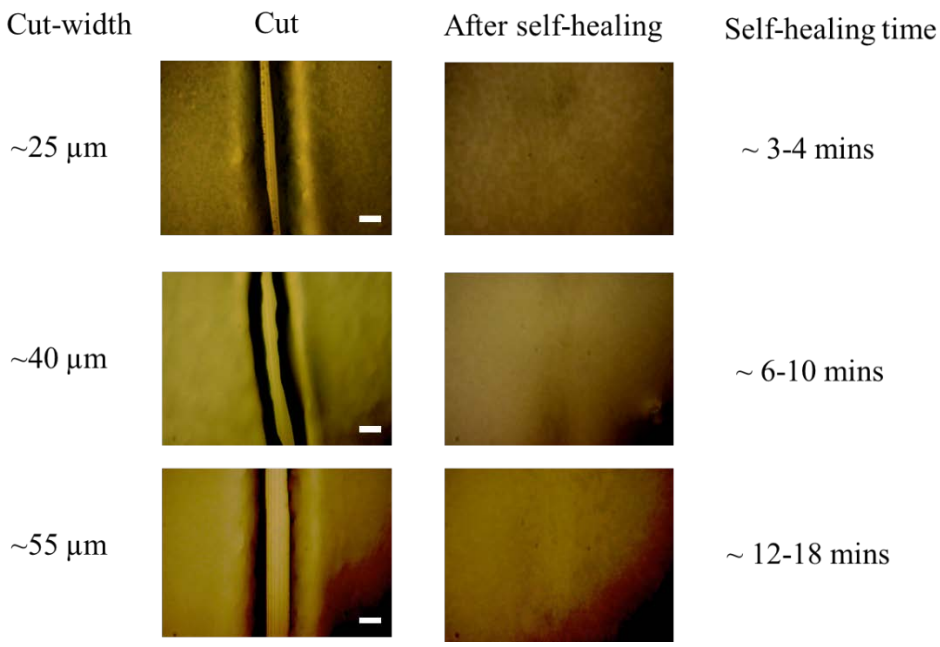

Fig. S9 Optical microscope images of PANI:PAAMPSA:PA samples during self-healing test (RH 90%). The scale bar is 50 µm.

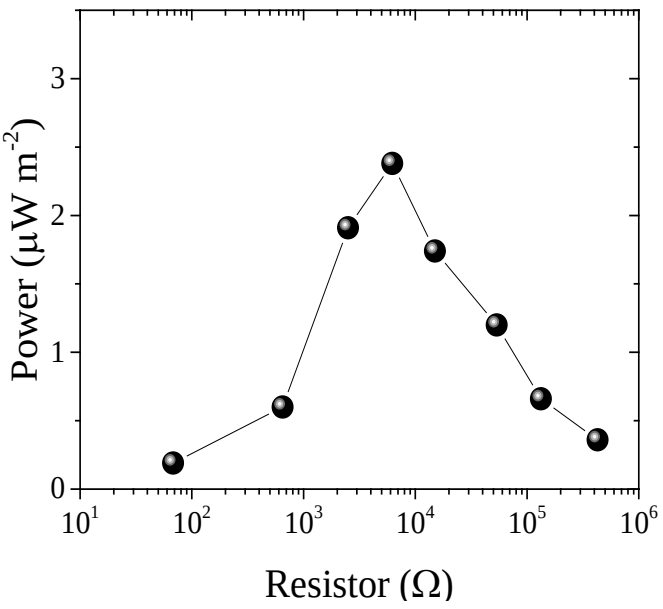

Fig S10 The power output of the PANI:PAAMPSA:PA with different resistors at ΔT of 1.7 K.

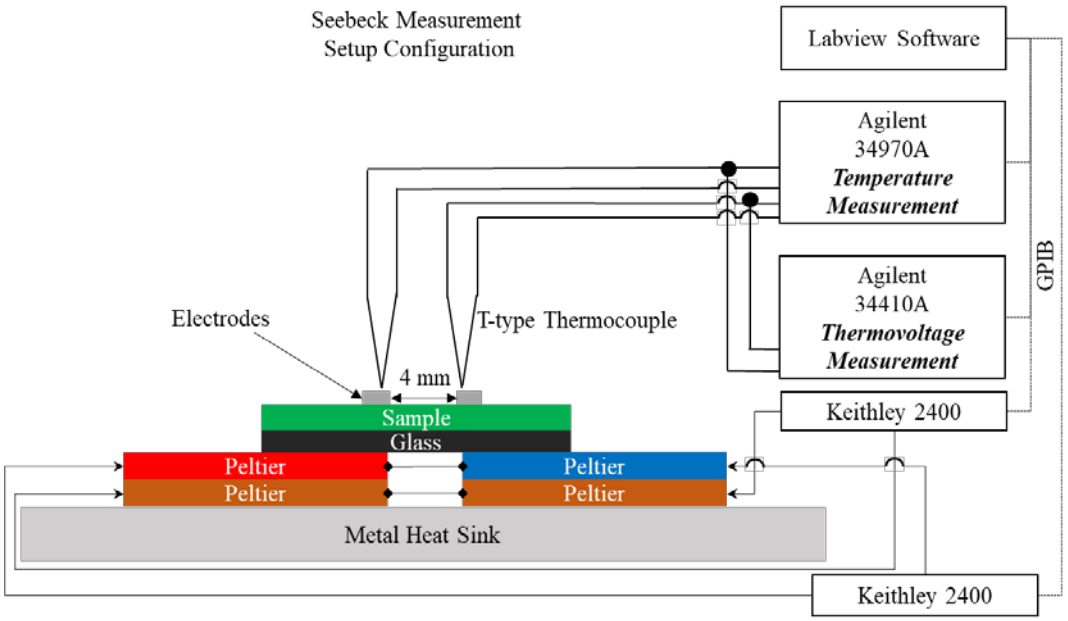

Fig. S11 A schematic description of the Seebeck coefficient measurement.

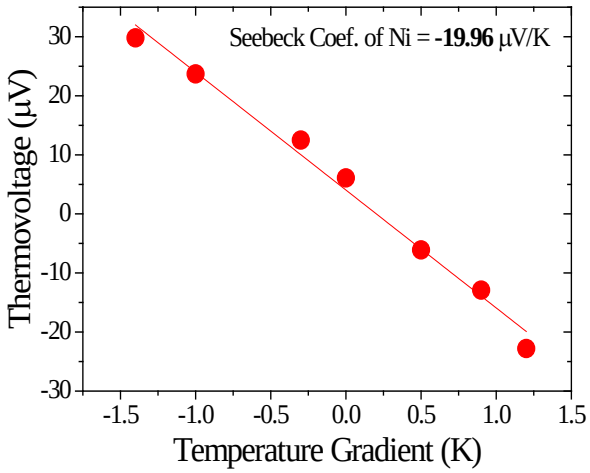

Fig. S12 Thermovoltage of a nickel plate as a reference for Seebeck coefficient measurement.

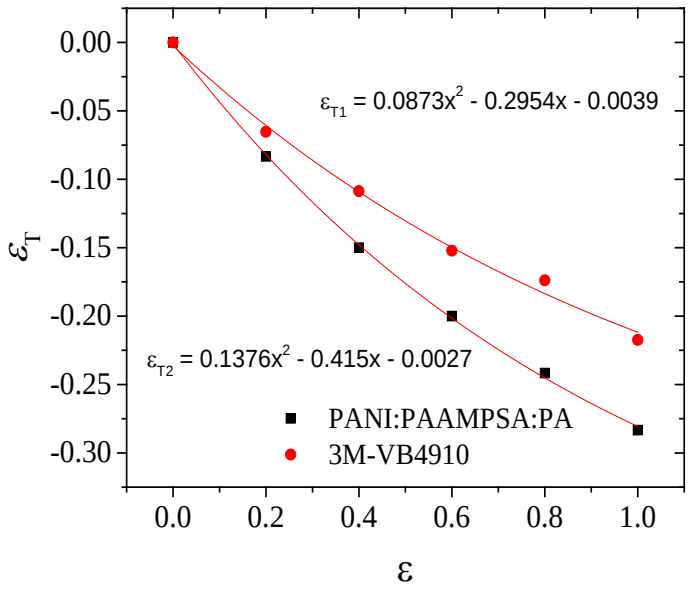

Fig. S13. The experimentally determined contraction in width (transverse strain, ε_T) of 3M-substrate and PANI:PAAMPSA:PA samples as a function of longitudinal strain, ε, as well as a quadratic function $\varepsilon_T(\varepsilon)$. The lines indicate the fitting of the data.

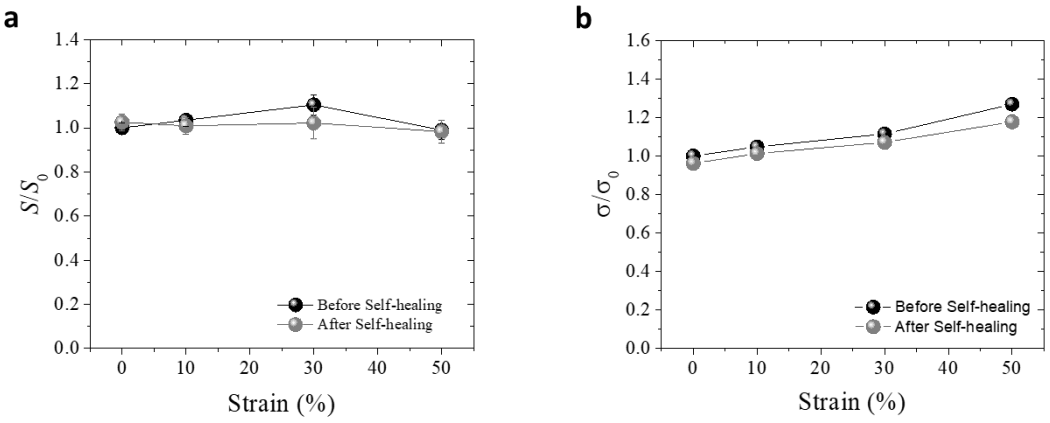

Fig. S14 The (a) Seebeck coefficient and (b) electrical conductivity of PANI:PAAMPSA:PA under different strain condition, before and after self-healing process.

Table S1 Young's Moduli, strength, and toughness of PANI:PAAMPSA:PA, PAAMPSA:PA, and PANI:PAAMPSA.

Sample	PANI:PAAMPSA:PA				PAAMPSA:PA	PANI:PAAMPSA
Relative Humidity (% RH)	30	40	60	80	40	40
Young's Moduli (kPa)	1106	178	38	11	1121	980
Strength (MPa)	2.85	0.55	0.42	0.35	2.18	1.34
Toughness (MJ/m^3)	235	138	161	157	43	165

Table S2 Composition of nitrogen- and sulfur-containing functional groups based on peak area from XPS spectra of PAAMPSA, PANI:PAAMPSA, and PANI:PAAMPSA:PA with deconvoluted N 1s and S 2p peaks in Fig. S5. The % ratios were calculated by comparing the areas of the peaks.

Sample	N 1s			S 2p	
	NH (%)	N^+ (%)	N_2^+ (%)	$-SO_3^-$ (%)	$-SO_3H$ (%)
PAAMPSA	-	-	-	75.0	25.0
PANI:PAAMPSA	26.0	26.5	47.5	48.5	51.5
PANI:PAAMPSA:PA	22.6	15.1	62.3	25.8	74.2

Table S3 Thermoelectric properties of the TE hybrids with different PA content.

Sample	***S*** **(mV K^{-1})**	**σ_i (S cm^{-1})**	**PF_i (mW m^{-1} K^{-2})**
PAAMPSA	5.7 mV K^{-1}	-	-
PANI (11wt%): PAAMPSA (83wt%): PA (6wt%)	7.8 mV K^{-1}	0.19	1.2
PANI (9wt%): PAAMPSA (68wt%): PA (23wt%)	8.1 mV K^{-1}	0.24	1.6
PANI (7wt%): PAAMPSA (56wt%): PA (37wt%)	8.2 mV K^{-1}	0.25	1.7

Table S4 Thermal conductivities and water content of the TE hybrids at various humidity levels.

Humidity (% RH)	40	50	60	70	80	90
Total weight of the sample (g)	0.2255	0.2416	0.2553	0.2679	0.2939	0.3212
Relative weight of absorbed water in the sample (g)	0	0.016	0.030	0.042	0.068	0.096
Volume fraction of absorbed water	0	0.095	0.163	0.217	0.309	0.384
Sample density (g cm^{-3})	1.467	1.422	1.391	1.366	1.323	1.288
Thermal conductivity (W m^{-1} K^{-1})	0.358	0.381	0.397	0.410	0.432	0.451

References

1. 1 A. T. Burkov, A. Heinrich, P. P. Konstantinov, T. Nakama, K. Yagasaki, *Meas. Sci. Technol*., 2001, **12**, 264.
2. S. Kee, H. Kim, S. H. K. Paleti, A. El Labban, M. Neophytou, A. H. Emwas, H. N. Alshareef and D. Baran, *Chem. Mater*., 2019, **31**, 3519–3526.
3. D. J. Lipomi, J. A. Lee, M. Vosgueritchian, B. C. K. Tee, J. A. Bolander and Z. Bao, *Chem. Mater*., 2012, **24**, 373–382.
4. F. Jiao, A. Naderi, D. Zhao, J. Schlueter, M. Shahi, J. Sundström, H. Granberg, J. Edberg, U. Ail, J. Brill, T. Lindström, M. Berggren and X. Crispin, *J. Mater. Chem. A*, 2017, **5**, 16883–16888.
5. D. Zhao, H. Wang, Z. U. Khan, J. C. Chen, R. Gabrielsson, M. P. Jonsson, M. Berggren, X. Crispin, *Energy Environ. Sci.*, 2016, **9**, 1450-1457.